HHS Public Access

Author manuscript

J Autoimmun. Author manuscript; available in PMC 2022 April 22.

Published in final edited form as:

J Autoimmun. 2021 August ; 122: 102677. doi:10.1016/j.jaut.2021.102677.

Novel autoantibodies to the β-cell surface epitopes of ZnT8 in patients progressing to type-1 diabetes

Yong Gu[1], **Chengfeng Merriman**[3], **Zheng Guo**[3], **Xiaofan Jia**[1], **Janet Wenzlau**[1], **Hua Li**[2], **Huilin Li**[2], **Marian Rewers**[1], **Liping Yu**[1,**], **Dax Fu**[3,**]

[1]Barbara Davis Center for Diabetes University of Colorado School of Medicine, Aurora, CO

[2]Department of Structural Biology, Van Andel Institute, Grand Rapids, MI

[3]Department of Physiology, Johns Hopkins School of Medicine, Baltimore, MD

Abstract

Type 1 diabetes (T1D) is a chronic autoimmune disease characterized by autoimmune destruction of insulin-producing β-cells in pancreatic islets. Seroconversions to islet autoantibodies (IAbs) precede the disease onset by many years, but the role of humoral autoimmunity in the disease initiation and progression are unclear. In the present study, we identified a new IAb directed to the extracellular epitopes of ZnT8 (ZnT8ec) in newly diagnosed patients with T1D, and demonstrated immunofluorescence staining of the surface of human β-cells by autoantibodies to ZnT8ec (ZnT8ecA). With the assay specificity set on 99th percentile of 336 healthy controls, the ZnT8ecA positivity rate was 23.6% (74/313) in patients with T1D. Moreover, 30 children in a longitudinal follow up of clinical T1D development were selected for sequential expression of four major IAbs (IAA, GADA, IA-2A and ZnT8icA). Among them, 10 children were ZnT8ecA positive. Remarkably, ZnT8ecA was the earliest IAb to appear in all 10 children. The identification of ZnT8ec as a cell surface target of humoral autoimmunity in the earliest phase of IAb responses opens a new avenue of investigation into the role of IAbs in the development of β-cell autoimmunity.

Islet autoantibodies (IAbs) are currently the most reliable biomarkers used for differential diagnosis and prediction of type-1 diabetes (T1D), but they are generally considered as bystanders in the disease progression leading to T cell-mediated autoimmune destruction of β-cells. It is well established that autoantibodies to antigenic targets on the cell surface are pathogenic mediators in a group of autoimmune diseases including Graves' disease and myasthenia gravis (1). Islet Cell-Surface Autoantibodies (ICSA) in T1D were first described in 1970's (2,3), examined for lytic effects on pancreatic β-cells (4), but contradictory results came from multiple study groups (5,6). Until now, ICSAs have never been defined biochemically, and the molecular target of putative ICSAs remains unidentified. T1D is a chronic autoimmune disease that often starts in childhood (7). While most patients are diagnosed many years after seroconversion to IAbs (8), the initial factors involved in the

[**]**Address correspondence to:** Liping Yu, Barbara Davis Center for Diabetes University of Colorado School of Medicine, Aurora, CO. Phone: 303-724-6842; Liping.Yu@cuanschutz.edu, Dax Fu, Department of Physiology, Johns Hopkins School of Medicine, Baltimore, MD. Phone: 443-287-4941; dfu3@jhmi.edu.

early phase of the pathological cascade are still unclear due to their elusive chronic effects. IAbs are secreted by plasma cells derived from autoreactive B-cells. NOD mice lacking B cells are resistant to T1D (9,10), and depleting B cells delays disease progression in both animal models and human clinical trials (11,12). These findings support the notion that disease-associated autoantibodies might play a role in the development of T1D (13). However, all well-established IAbs recognize intracellular antigens and secreted insulin. The lack of biochemically defined ICSAs is one of the critically missing links in understanding the pathogenic role of humoral autoimmunity.

Zinc transporter-8 (ZnT8) is a major self-antigen in T1D (14). It is a two-modular membrane protein consisting of a major transmembrane domain (TMD) and a cytosolic module formed by a tight association of a C-terminal domain (CTD) and a N-terminal domain (NTD) (15). All currently tested autoantibodies to ZnT8 are limited to ZnT8 intracellular epitopes (ZnT8ic) localized to CTD. NTD is a minor antigen, contributing to ~8% of overall ZnT8icAb-reactivity with ~99% overlap with the CTD-reactivity (16). By comparison, TMD is more than twice the size of CTD, suggesting that a significant portion of antigenicity may arise from the ZnT8 extra-cellular epitopes (ZnT8ec) of TMD (Fig. 1A). Moreover, ZnT8 is one of the most abundantly expressed membrane proteins in human β-cells (17), and its subcellular distribution is functionally coupled with insulin secretion, biosynthesis and storage (18,19). Glucose stimulated insulin secretion promoted the display of ZnT8 on the surface of live β-cells, making it a potential target for ICSA recognition (20). Our previous comparative analyses of ZnT8 autoantibodies to CTD and a full-length ZnT8 splice isoform (TMD+CTD) raised a possibility that autoantibody to ZnT8ec (ZnT8ecA) might exist (21,22), but a direct biochemical identification of ZnT8ecA remained unattainable due to the lack of a definitive assay for conformation-specific serum antibodies to ZnT8ec.

High-affinity binding of autoantibodies to conformational epitopes on the cell surface is a key driver of autoantibody-induced pathology (23). Linear peptides in the absence of a protein scaffold do not form structurally-defined conformational epitopes while the purified ZnT8 by itself is highly unstable in maintaining its native folding. In the present study, we generated natively folded human ZnT8 in a novel stabilizing protein complex, and developed an electrochemiluminescence (ECL)-assay to identify ZnT8ecA biochemically in newly diagnosed patients with T1D. We also demonstrated direct accessibility of ZnT8ec epitopes to extracellular IAbs by ZnT8-specific immunofluorescence staining on the surface of human β-cells. By comparison, the accessibility of ZnT8ic epitopes to IAbs requires prior cell damage that releases intracellular antigens to the extracellular space (24), resulting in secondary events of epitope spreading during the procession of islet autoimmunity (25). Hence, we further examined the temporal relationship of multiple IAb seroconversions in a selected cohort of young children who developed all four major IAbs. A longitudinal follow-up analysis of these children from birth to clinical T1D revealed that ZnT8ecA was the earliest IAb to appear in all children tested, followed by IAbs to insulin (IAA), glutamic acid decarboxylase-65 (GADA), protein tyrosine phosphatase-related islet antigen-2 (IA-2A), and ZnT8ic (ZnT8icA), respectively. The identification of ZnT8ecA as a major ICSA and demonstration of intramolecular epitope spreading from cell surface ZnT8ec to intracellular ZnT8ic epitopes suggest a potential role of antibody-mediated β-cell damage in the early phase of humoral autoimmunity development.

Materials and Methods

Serum samples

Two independent groups of serum samples from newly diagnosed patients with diabetes mellitus were used in the ECL-ZnT8ecA assay. The demographic information of these samples for each group are summarized in Tabel-1. All patients were diagnosed at Barbara Davis Center for Diabetes, and serum samples were obtained from patients within two weeks of diagnosis. Age and gender matched healthy control samples were included for each experimental patient group in the study. In addition, samples from 30 children from the Diabetes Auto Immunity Study in the Young (DAISY) who were longitudinally followed from birth to clinical T1D were used in the study. All samples from patients with diabetes and healthy controls were previously tested for all four established IAbs with RBA. The samples from 30 longitudinally followed children were tested for IAbs with both RBA and ECL assay. Signed written informed consents were obtained from participants and the studies were approved by the Institutional Review Board of the University of Colorado.

ZnT8-Fab complex

The human ZnT8 isoform-2 cDNA (NM_001172814.1) was subcloned into a mammalian pCMV6-based expression vector (26). The expression plasmid was introduced into FreeStyle 293-F cells, transiently expressed in suspension culture, and purified as described previously (21,26). mAb20 and mAb39 were produced by hybridoma cells grown in BD quanta medium plus 10% ultralow-IgG FBS. After 3–4 weeks of cell culture, mAb20 and mAb39 in the culture medium were captured by protein A/G beads (Thermo), washed with PBS, and then eluted by an IgG elution buffer (Thermo). The purified mAbs were concentrated to ~20 mg/ml for Fab production using a Piercers Fab preparation kit following manufacturer's protocol. The resulting Fab20 or Fab39 was HPLC purified in PBS, labeled with Sulfo-tag, and then HPLC purified again to remove free sulfo-tag in the reaction mixture. Finally, purified Fabs were mixed with ZnT8 in 10:1 molar ratio, incubated overnight, and then the resultant ZnT8-Fab20-Fab39 ternary complex or ZnT8-Fab20 binary complex was purified by sizing HPLC as a single monodisperse protein peak. The purified ternary complex with sulfo-tag was used for ZnT8ecA detection while the purified binary complex without sulfo-tag was used for cryo-EM single particle analysis.

Cryo-EM and 3D reconstruction

Freshly glow discharged Quantifoil R 1.2/1.3 gold grids (300 mesh) were prepared by double blotting of HPLC-purified ZnT8-Fab20 protein complex in 3.0 mg/ml. Each blotting was done for 3 s at 6 ℃ and 100% relative humidity. After the second blotting, the grids were plunge-frozen in liquid ethane using a Vitrobot Mark III. Cryo-EM data were collected automatically with EPU in a FEI Talos Arctica transmission electron microscope operated at 200 kV. A total of 484 movies were recorded on a Falcon 3EC in linear mode at a magnification of 130,000, equivalent to a pixel size of 1.21 Å. Each movie consists of 40 frames with a total dose of 62 $e^{-}/Å^{2}$ for a total exposure time of 2 s. Defocus values varied from −1.5 to −2.5 μm. Raw movies were motion-corrected by MotionCor2 (27), and then CTFFIND4.1.8 was used to estimate the contrast transfer function parameters for each micrograph (28), which was processed by RELION2.1.0 (29). Specifically, about

1,000 particles were manually picked and were subjected to reference-free 2D classification. Five out of ten representative 2D class averages were used as templates for automatic particle-picking. A total of 64,920 particles were picked and were sorted by three rounds of 2D classification. 55,396 particles in those classes with good features were retained and were subjected to 3D classification. Based on visual inspection, 36,345 particles belonging to three classes with structural features combined for further refinement. A C2 symmetry was applied during final 3D reconstruction and refinement, resulting in the reported 3D map at a nominal resolution of 17 Å, based on the gold standard Fourie shell correlation between two half maps.

Structural modeling

A monoclonal Fab (PDB ID: 1M71) as a Fab homologue model and cryo-EM structure of human ZnT8 (PDB ID: 6XPD) were docked into the 3D map of ZnT8-Fab20. Rigid-body docking was performed using UCSF Chimera (30). For the ZnT8ecA-ZnT8-Fab20-Fab39 complex, an intact IgG2a monoclonal antibody (PDB ID: 1IGT) as a ZnT8ecA homologue on the extracellular surface of TMD, Fab molecules (PDB ID: 1M71) and the cryo-EM structure of human ZnT8 (PDB ID: 6XPD) were docked as rigid-body into the 3D map of ZnT8-Fab20-Fab39 (31).

ZnT8ecA assay

Assay components are schematically represented in Fig. 1B with a workflow as following. First, a serum (10μl) was mixed with 25 μl of HPLC-purified ZnT8-Fab20-Fab39 ternary complex with a Sulfo-tag at a final concentration of 500 ng/ml in PBS (pH 7.4) plus 0.005% lauryl maltose neopentyl glycol (LMNG). The mixture was incubated at room temperature for 1 h on a plate shaker. Then 5 μl of 25 μg/ml biotinylated anti-(human IgG)-Fc mAb (Thermo Scientific) was added to the mixture and incubated at room temperature for 1 h with shaking. Meanwhile, 96-well streptavidin-coated ECL plates were blocked with 150 μl of 3% Blocker A (MSD) per well. The blocked ECL plate was 3x washed with PBS plus 0.005% LMNG, followed by the addition of the incubated serum-antigen, anti-IgG mixture into the ECL plate. After incubation at room temperature for 1 h, the plate was washed three times with PBS plus 0.005% LMNG to remove uncaptured antigen-antibody complex. Finally, 150μl/well of 2× reading buffer (MSD) were added and the plate was counted on an ECL Sector SQ120 (Meso-Scale Discovery). An internal standard positive and a negative control serum samples were used to normalize the assay readout as an index (index=$(\text{Signal}_{\text{sample}}-\text{Signal}_{\text{negative-control}})/(\text{Signal}_{\text{positive-control}}-\text{Signal}_{\text{negative-control}})$. Median years of first seroconversion and their distributions for each IAb in 10 DAISY subjects were shown in a box-and-whisker plot by SigmaPlot. The levels of statistic difference between the median years seroconverted to ZnT8ecAb and other IAbs were measured by *P* values as exact solutions of the two-sided Wilcoxon-Mann-Whitney test for paired data sets (32).

RBAs for IAA, GADA, IA-2A and ZnT8icAb were published previously. Briefly, RBA for GADA and IA-2A were performed with NIH/NIDDK harmonized standard methods (33). RBA for IAA and ZnT8icA were performed with in-house assays (14,34). In the most recent

IASP Workshop of 2020, the sensitivity and specificity were 78% and 99% for GADA, 72% and 100% for IA-2A, 62% and 99% for IAA, 74% and 100% for ZnT8icAb.

Immunofluorescence staining and imaging

A droplet (20 μl) of ~2000 human insulinoma cells (EndoC-βH1) was seeded onto a glass bottom microwell dish that was pre-coated with β-coat (Univercell-Biosolutions). After cell adhesion to the surface, 2 ml OPTI cell culture medium (Univercell-Biosolutions) was added to the dish, and cells inside the well were grown at 37 °C in a 5% CO_2 humidified atmosphere for two days. At this time, cells were washed with a high glucose (20 mM) Krebs buffer, and then fixed using a flowcytometry fixation buffer (R&D) for 20 min at RT, washed again using PBS plus 1% BSA. Next, 10 μl human serum diluted in 90 μl PBS was added to the microwell to cover EndoC-βH1 cells, incubated for 4 hr at RT. Unbound serum antibodies were removed by 2x wash using PBS plus 1% BSA, and then an Alexa Fluor-647 conjugated anti-human IgG antibody (Life technologies, dilution 1:1000) in 100 μl PBS+1%BSA was added to the microwell, incubated for 1 hr at RT. Finally, cells were washed with PBS to remove unbound secondar antibody, and then sealed under a drop of mounting solution with DAPI for fluorescence imaging on a Zeiss LSM 700 inverted confocal microscope with a 63x oil objective. For serum pre-absorption, human ZnT8-GFP was stably expressed in rat insulinoma cells (INS-1E) where ZnT8-GFP was abundantly displayed on the cell surface as described earlier (20). 5×10^4 INS-1E cells with ZnT8-GFP over-expression were grown in a 96-well plate, fixed using a flowcytometry fixation buffer, and then exposed to 100 μl diluted sera to absorb serum ZnT8ecA. After an overnight incubation at 4 °C, sera were recovered for later immunofluorescence staining of human EndoC-βH1 cells as described above. Alternately, recombinant human ZnT8 was transiently expressed in FreeStyle 293-F cells, purified and reconstituted into proteoliposomes as described earlier (26). Proteoliposomes containing 0.1 mg of purified ZnT8 was pelleted by ultracentrifugation, resuspended in 100 μl diluted sera to absorb serum ZnT8 autoantibody. After an overnight incubation at 4 °C, sera were recovered by ultracentrifugation to remove ZnT8 proteoliposomes. The resultant supernatants were used for immunofluorescence staining of human EndoC-βH1 cells as described above.

Results

Stable ZnT8-Fab complex

To stabilize the native ZnT8 conformation for ZnT8ecA binding and to block ZnT8icA binding, we used antigen-binding fragments (Fabs) of two ZnT8ic monoclonal antibodies, mAb20 and mAb39, to form a stable binding complex. Earlier functional characterization of mAb20 and mAb39 established sub-nanomolar binding affinities for both mAbs and demonstrated the stable formation of a ZnT8-Fab20-Fab39 ternary complex (31). This ternary complex was HPLC-purified and adapted to an ECL-based ZnT8ecA assay (Fig. 1B) (35). The native ZnT8 conformation and spatial arrangements of multiple Fabs around a ZnT8 homodimer were revealed by single-particle electron microscopy (EM) and protein docking analysis. The ZnT8ecA was modeled by docking an immunoglobulin-G molecule to the extracellular surface of a cryo-EM structure of human ZnT8 at 3.8-angstrom resolution (15), Fab20 by docking a Fab molecule to the electron density of a ZnT8-Fab20 complex

at 17-angstrom resolution (Fig. 1C), and Fab39 by docking a Fab molecule to the electron density of a ZnT8-Fab20-Fab39 complex as reported earlier (31). The co-bindings of Fab20 and Fab39 were found to shield the surface of cytoplasmic domains while the detergent micelle surrounded the transmembrane sector of TMD (Fig. 1C). Lipid molecules with a strong association with the hydrophobic surface of TMD may exist in the detergent ring, but they are immunologically silent because ZnT8 was produced from over-expression in human cells. Thus, the extracellular surface of TMD was an only option for ZnT8ecA binding to the ternary protein complex (Fig. 1A). To minimize ZnT8icA binding to NTD, we used a native ZnT8 splice variant that reduces the NTD to a 13-aa peptide (36). This N-terminal sequence was secluded in a crevice between two CTDs (15). Fab39 was docked to the CTD-CTD interface, blocking potential ZnT8icA access to NTD. Fab20 was docked to a different CTD surface in a direction approximately parallel to the membrane surface (Fig. 1C), posing steric hindrance to potential ZnT8icA binding to the intracellular surface of TMD. Taken together, co-bindings of Fab20 and Fab39 effectively protected NTD, CTD and the intracellular surface of TMD from ZnT8icA binding, allowing specific detection of ZnT8ecA on the electrode surface of ECL-sensors (Fig. 1B).

Identification of ZnT8ecA.

To further ensure a specific detection of ZnT8ecA, we generated two polymorphic ZnT8 variants in ZnT8-Fab20-Fab39 ternary complexes, and examined the cross-reactivity of individual serum samples to each of the two ZnT8 variants. It is well established that the epitope specificity of ZnT8icA is determined by a nonsynonymous single nucleotide polymorphism, which causes an arginine (R) to tryptophan (W) change at position 325 of CTD (16,31). Sera from R-homozygous patients do not cross-react with the W-form ZnT8ic epitopes, whereas sera from W-homozygous patients do not cross-react with the R-form ZnT8ic epitopes. Sera from R/W heterozygous patients can react with both R- and W-form ZnT8ic epitopes. Since ZnT8ec epitopes on the surface of TMD is independent of polymorphic variations in CTD, a *bona fide* ZnT8ecA is expected to cross-react with both ZnT8-R and ZnT8-W antigens. All serum samples examined were pre-screened by radio-binding assay (RBA) with two CTD variants to exclude sera that exhibited cross-reactivity to polymorphic ZnT8ic epitopes. Of 300 ZnT8icA-postive sera from new onset patients with T1D, we identified 94 serum samples lacking ZnT8icA cross-reactivity, including 49 exclusively positives for R-form CTD (R-sera), and 45 for W-form CTD (W-sera) (Fig. 2A). Additional sera included in the present study were 35 samples from new onset patients with T1D negative for ZnT8icA but positive for other IAbs, and 22 from new onset diabetic patients (presumptive type-2 diabetes) negative for all IAbs. In all selected patients examined for R/W cross-reactivity (Fig. 2B), ZnT8ecA was detected positive in 31% (29/94) of patients with T1D who were also positive for ZnT8icA (including 16/49 R-sera and 13/45 W-sera), in 23% (8/35) of patients with T1D who were negative for ZnT8icA, and in 4.5% (1/22) of diabetic patients who were negative for all IAbs (Fig. 2C). The assay cutoff level for ZnT8ecA positivity was set on 99th percentile in 197 healthy controls from general population with matched ages and genders (Fig. 2C).

Validation of ZnT8ecA assay.

To confirm the results of the ZnT8ecA assay, an independent second group of 449 samples were tested, including 184 new onset patients with T1D who were positive for IAbs (123 positive and 61 negatives for ZnT8icA), 126 new onset diabetic patients negative for all IAbs (presumptive type-2 diabetes), and 139 age/gender matched healthy controls. Similarly, two polymorphic variants of the ZnT8-Fab20-Fab39 ternary complex (R-form and W-form) were tested for R/W cross-reactivity. All sera positive for ZnT8icA were pre-screened and selected for exclusive reactivity to either ZnT8ic-R or ZnT8ic-W antigen. With the assay specificity set on 99th percentile of 139 healthy controls (2/139), the ZnT8ecA positivity rate was 20.1% (37/184) in patients with T1D including patients positive for ZnT8icA (19/123) and patients negative for ZnT8icA (18/61). In addition, the ZnT8ecA positivity rate was 4.8% (6/126) in diabetic patients (presumptive T2D) negative for all IAbs (Fig. 2D). Taken together, the two independent serum sets collectively gave a ZnT8ecA positivity rate of 23.6% (74/313) and an assay specificity of 99% (3/336) in patients with T1D. ZnT8ecA appeared independent of ZnT8icA with a similar positivity rate in new onset patients with or without ZnT8icA. Among 313 T1D cases enrolled in the present study, 46 adults in total but only one at the age of 20 developed low ZnT8ecA positivity. The ZnT8ecA positivity rate at 27.3% (73/267) in children was significantly higher ($P < 0.0001$) than that in adults (1/46). The observed age-dependency of ZnT8ecA is similar to that of IAA, which tends to develop in children with more aggressive autoimmunity as compared with adult-onset T1D.

ZnT8ecA binding on the surface of human β-cells.

ZnT8 is abundantly expressed in human EndoC-βH1 β-cells with an expression level similar to that of the housekeeping α-tubulin at the protein level (18). We examined immunofluorescence staining of intact EndoC-βH1 cells using individual human sera tested either positive or negative for ZnT8ecA. Sera from healthy controls exhibited a negligibly low level of surface staining. ZnT8ecA(+)/ZnT8icA(+) and ZnT8ecA(+)/ZnT8icA(−) sera from patients with T1D showed an elevated level of surface staining as compared with that of ZnT8ecA(−)/ZnT8icA(+) and ZnT8ecA(−)/ZnT8icA(−) sera (Fig. 3A). To demonstrate ZnT8-specific cell surface staining, we generated stable expression of human ZnT8-GFP in rat INS-1E β-cells (20), and then used ZnT8-GFP displayed on the cell surface to absorb serum ZnT8ecA (20). Pre-absorption of human sera abolished surface immunofluorescence staining of EndoC-βH1 cells (Fig. 3B). We further purified human ZnT8 and reconstituted it into proteoliposomes that was used to pull-down serum ZnT8ecA and ZnT8icA by ultracentrifugation. A trace amount of detergent molecules from the proteoliposome preparation caused membrane leakage during immunofluorescence staining of EndoC-βH1 cells. Proteoliposome pre-absorption of human sera yielded intracellular staining, but completely abolished the ring-like profile of cell surface staining (Fig. 3C). This finding indicated that ZnT8ecA predominantly contributed to cell surface staining whereas residual IAbs in proteoliposome-absorbed sera caused intracellular staining as a result of β-cell damage. Interestingly, ZnT8ecA(−)/ZnT8icA(−) sera from patients with presumptive T2D exhibited no or lower levels of intracellular IAb staining (Fig. 3C).

Early expression of ZnT8ecA in pre-T1D young children.

The timing of seroconversions to ZnT8ecA and ZnT8icA may differ due to the difference in the immunological accessibility of respective epitopes before and after β-cell damage. To examine this hypothesis, we selected 30 DAISY children who sequentially developed four major IAbs before overt disease. All 30 children were longitudinally followed from birth to clinical T1D, and 10 were tested positive for ZnT8ecA (Fig 4A). Of these ZnT8ecA(+) children, seven were detected ZnT8ecA first, earlier than any other IAbs. The remaining three children were detected ZnT8ecA, IAA and/or GADA first at the same time. The time distributions of IAb onsets in these children are shown in a cumulative positivity plot (Fig. 4B), and median times of individual IAb seroconversions, their distributions and variability are summarized in a box and whisker plot (Fig. 4C). The median times were 1.2, 2.1, 2.2, 2.6 and 5.5 years for the first appearance of ZnT8ecA, IAA, GADA, IA-2A and ZnT8icA, respectively. Two-sided Wilcoxon-Mann-Whitney tests for paired datasets indicated that the first seroconversion to ZnT8ecA was marginally earlier than IAA and GADA (P=0.052), but significantly earlier than IA-2 (P=0.005) and ZnT8icA (P=0.002) (Fig. 4C). Our results indicated that the rank order of IAb first appearance was ZnT8ecA<IAA≈GADA<IA2A<ZnT8icA in 10 DAISY children studied. Of note, the onsets of ZnT8ecA and ZnT8icA exhibited a median delay of 4.3 years.

Discussion

It is generally accepted that the first autoantibody appearance with seroconversion to multiple IAbs marks the initiation of islet autoimmunity (8,37), but the lack of biochemically defined ICSAs on the β-cell surface impedes investigation into the potential pathogenic role of IAbs in the development of humoral autoimmunity. Here we report the identification of a new IAb to extracellular epitopes of ZnT8 on the β-cell surface. ZnT8ecA recognizes both ZnT8 polymorphic variants, and is the first seroconverted IAb in all 10 DAISY children studied whereas ZnT8icA is polymorphism-specific, and a later IAb closer to the disease onset. The distinctive timing of ZnT8ecA appearance and its cell surface binding suggest that ZnT8ecA represents a novel autoantibody category independent of classical IAbs. Notably, ZnT8ecA was detected by a median of 0.9 years earlier than IAA, which often appears as the first autoantibody among very young children (38). Seroconversion to autoantibody positivity at an early age is associated with an increased risk for progression to clinical T1D (39). The earliest appearance of ZnT8ecA would allow for a more precise detection of islet autoimmunity onset. Hence, the potential of ZnT8ecA as a biomarker for earlier detection of islet autoimmunity is of clinical importance to risk prediction and disease prevention.

The early appearance of ZnT8ecA suggests a potential role of ZnT8 in triggering islet autoimmunity. Insulin/proinsulin has been implicated as a primary self-antigen in the HLA DR4-DQ8-positive form of T1D (40), but secreted insulin molecules do not mediate cell surface binding of IAA with cytotoxic effects. In contrast, the observed ZnT8-specific, cell surface immunofluorescence staining was attributed to ZnT8ecA binding to ZnT8ec epitopes on the surface of human β-cells, in agreement with earlier flow cytometry quantification of ZnT8-specific cell surface staining with pooled sera from patients with T1D (21). The

identification of ZnT8ecA as a major ICSA provides an experimental basis for further investigation into ZnT8ecA-mediated antibody-dependent cellular cytotoxicity (ADCC) and complement-dependent cytotoxicity (CDC). The immunological stress resulted from ZnT8ecA-ZnT8ec interactions on the cell surface is in line with the emerging notion that β-cell stress is central to T1D pathogenesis (41).

The presence of serum ZnT8ecA may reflect the activation of ZnT8-autoreactive B cells that undergo clonal expansion and differentiation into antibody-secreting plasma cells. Mature naive B cells could infiltrate into pancreatic islets where a continuous exposure of the B cell receptors (BCR) to cell surface antigens could activate B cell proliferation (42). The large gap in the responses of ZnT8ecA and ZnT8icA suggests an earlier propagation of ZnT8-autoreactive B cell clones upon BCR-recognition of ZnT8ec epitopes on the cell surface. Likewise, the extracellular insulin availability may explain how IAA arises as one of the earliest IAbs before severe autoimmune destruction of β-cells (43). On the other hand, ZnT8ic is an intracellular antigenic domain whose BCR-recognition is only in conditions of cell damage that releases ZnT8ic epitopes to the extracellular environment. Hence, B cells with BCRs that recognize ZnT8ic are expected to propagate later than those that react with ZnT8ec on the cell surface, explaining a delayed seroconversion to ZnT8icA.

Recently, IAbs to the extracellular domain of IA-2 (IA2ecA) were identified in a small portion of diabetic patients (44). While IA-2 and ZnT8 are both associated with the insulin secretory granule, only ZnT8 was shown trafficked to the cell surface upon glucose stimulation (20). It remains uncertain as to whether IA-2 can be surfaced (45,46). In addition, IA-2A like many other T1D-associated IAbs targets self-antigens that are ubiquitously expressed. By comparison, the tissue distribution of ZnT8 is islet-specific (47). *ZnT8* (*SLC30A8*) mRNA was limited to all five endocrine cell types (α, β, γ, δ and ε cells) in islets of Langerhans, but not detected in exocrine ductal and acinar cells (17). Given strong differences between mRNA and protein quantities within and across human tissues (48), the relative protein abundance of ZnT8 in different types of endocrine cells may be more reliably reflected by the zinc transport activity. ZnT8 predominantly functions as a zinc sequestering transporter in the insulin secretory vesicles of β-cells, which distinguishes from other endocrine cell types by an exceedingly high cellular zinc content (49). The dominant zinc transport activity of ZnT8 in β-cells and the identification of ZnT8ecA in patients with T1D support the β-cell specificity of ZnT8ecA actions on the cell surface where ZnT8 is dynamically linked to insulin secretion and production (50).

T1D is a heterogenous autoimmune disease with varied IAb responses depending on the HLA genotype, age and ethnicity (51–53). For example, the IAA prevalence is inversely associated with the age from a positivity rate of 80% in young children to only 20% in adults whereas the GADA prevalence increases with the age (51). The present study used sera from patients with mixed ages, thus the ZnT8ecA prevalence in different age groups and genetic backgrounds needs to be further studied. In addition, all patient sera in retrospective cohorts were collected shortly after the disease onset. The timing of serum collection may miss the ZnT8ecA peak, probably contributing to an underestimation of the ZnT8ecA positivity rate. A further study with large cohorts from patients with T1D as well as pre-diabetic subjects with longitudinal follow-up may be warranted.

Acknowledgments

This study was supported by the National Institutes of Health, R56 DK123435, RO1 DK032083, RO1DK032493, and Diabetes Research Center grant P30DK116073. Y. G., C. M., X. J., and J. W., performed autoantibody assays and data analysis; Z. G performed immunofluorescence staining and imaging analysis; H. L. and H. L. performed cryo-EM analysis and structural modeling; M. R. provided serum sample collection; L. Y. and D. F. are responsible for study design, data analysis and manuscript preparation. All authors contributed to manuscript revision. The authors declare no competing financial interests.

References

1. Tozzoli R (2020) Receptor autoimmunity: diagnostic and therapeutic implications. Auto Immun Highlights 11, 1 [PubMed: 32127047]
2. Lernmark A, Freedman ZR, Hofmann C, Rubenstein AH, Steiner DF, Jackson RL, Winter RJ, and Traisman HS (1978) Islet-cell-surface antibodies in juvenile diabetes mellitus. N Engl J Med 299, 375–380 [PubMed: 353557]
3. Van De Winkel M, Smets G, Gepts W, and Pipeleers D (1982) Islet cell surface antibodies from insulin-dependent diabetics bind specifically to pancreatic B cells. J Clin Invest 70, 41–49 [PubMed: 6123526]
4. Dobersen MJ, and Scharff JE (1982) Preferential lysis of pancreatic B-cells by islet cell surface antibodies. Diabetes 31, 459–462 [PubMed: 6759262]
5. Vives M, Somoza N, Soldevila G, Gomis R, Lucas A, Sanmarti A, and Pujol-Borrell R (1992) Reevaluation of autoantibodies to islet cell membrane in IDDM. Failure to detect islet cell surface antibodies using human islet cells as substrate. Diabetes 41, 1624–1631 [PubMed: 1446804]
6. Peterson C, Campbell IL, and Harrison LC (1992) Lack of specificity of islet cell surface antibodies (ICSA) in IDDM. Diabetes Res Clin Pract 17, 33–42 [PubMed: 1511659]
7. Atkinson MA, Eisenbarth GS, and Michels AW (2014) Type 1 diabetes. Lancet 383, 69–82 [PubMed: 23890997]
8. Ziegler AG, Rewers M, Simell O, Simell T, Lempainen J, Steck A, Winkler C, Ilonen J, Veijola R, Knip M, Bonifacio E, and Eisenbarth GS (2013) Seroconversion to multiple islet autoantibodies and risk of progression to diabetes in children. JAMA 309, 2473–2479 [PubMed: 23780460]
9. Serreze DV, Chapman HD, Varnum DS, Hanson MS, Reifsnyder PC, Richard SD, Fleming SA, Leiter EH, and Shultz LD (1996) B lymphocytes are essential for the initiation of T cell-mediated autoimmune diabetes: analysis of a new “speed congenic” stock of NOD.Ig mu null mice. J Exp Med 184, 2049–2053 [PubMed: 8920894]
10. Vong AM, Daneshjou N, Norori PY, Sheng H, Braciak TA, Sercarz EE, and Gabaglia CR (2011) Spectratyping analysis of the islet-reactive T cell repertoire in diabetic NOD Igmu(null) mice after polyclonal B cell reconstitution. J Transl Med 9, 101 [PubMed: 21722394]
11. Hu CY, Rodriguez-Pinto D, Du W, Ahuja A, Henegariu O, Wong FS, Shlomchik MJ, and Wen L (2007) Treatment with CD20-specific antibody prevents and reverses autoimmune diabetes in mice. J Clin Invest 117, 3857–3867 [PubMed: 18060033]
12. Pescovitz MD, Greenbaum CJ, Krause-Steinrauf H, Becker DJ, Gitelman SE, Goland R, Gottlieb PA, Marks JB, McGee PF, Moran AM, Raskin P, Rodriguez H, Schatz DA, Wherrett D, Wilson DM, Lachin JM, Skyler JS, and Type 1 Diabetes TrialNet Anti, C. D. S. G. (2009) Rituximab, B-lymphocyte depletion, and preservation of beta-cell function. N Engl J Med 361, 2143–2152 [PubMed: 19940299]
13. Smith MJ, Simmons KM, and Cambier JC (2017) B cells in type 1 diabetes mellitus and diabetic kidney disease. Nat Rev Nephrol 13, 712–720 [PubMed: 29038537]
14. Wenzlau JM, Juhl K, Yu L, Moua O, Sarkar SA, Gottlieb P, Rewers M, Eisenbarth GS, Jensen J, Davidson HW, and Hutton JC (2007) The cation efflux transporter ZnT8 (Slc30A8) is a major autoantigen in human type 1 diabetes. Proc Natl Acad Sci U S A. 104, 17040–17045. [PubMed: 17942684]
15. Xue J, Xie T, Zeng W, Jiang Y, and Bai XC (2020) Cryo-EM structures of human ZnT8 in both outward- and inward-facing conformations. Elife 9

16. Wenzlau JM, Liu Y, Yu L, Moua O, Fowler KT, Rangasamy S, Walters J, Eisenbarth GS, Davidson HW, and Hutton JC (2008) A common nonsynonymous single nucleotide polymorphism in the SLC30A8 gene determines ZnT8 autoantibody specificity in type 1 diabetes. Diabetes 57, 2693–2697 [PubMed: 18591387]

17. Segerstolpe A, Palasantza A, Eliasson P, Andersson EM, Andreasson AC, Sun X, Picelli S, Sabirsh A, Clausen M, Bjursell MK, Smith DM, Kasper M, Ammala C, and Sandberg R (2016) Single-Cell Transcriptome Profiling of Human Pancreatic Islets in Health and Type 2 Diabetes. Cell Metab 24, 593–607 [PubMed: 27667667]

18. Merriman C, and Fu D (2019) Down-regulation of the islet-specific zinc transporter-8 (ZnT8) protects human insulinoma cells against inflammatory stress. J Biol Chem 294, 16992–17006 [PubMed: 31591269]

19. Chimienti F, Devergnas S, Favier A, and Seve M (2004) Identification and cloning of a beta-cell-specific zinc transporter, ZnT-8, localized into insulin secretory granules. Diabetes 53, 2330–2337 [PubMed: 15331542]

20. Huang Q, Merriman C, Zhang H, and Fu D (2017) Coupling of Insulin Secretion and Display of a Granule-resident Zinc Transporter ZnT8 on the Surface of Pancreatic Beta Cells. J Biol Chem 292, 4034–4043 [PubMed: 28130446]

21. Merriman C, Huang Q, Gu W, Yu L, and Fu D (2018) A subclass of serum anti-ZnT8 antibodies directed to the surface of live pancreatic beta-cells. J Biol Chem 293, 579–587 [PubMed: 29184000]

22. Wan H, Merriman C, Atkinson MA, Wasserfall CH, McGrail KM, Liang Y, Fu D, and Dai H (2017) Proteoliposome-based full-length ZnT8 self-antigen for type 1 diabetes diagnosis on a plasmonic platform. Proc Natl Acad Sci U S A 114, 10196–10201 [PubMed: 28874568]

23. Ludwig RJ, Vanhoorelbeke K, Leypoldt F, Kaya Z, Bieber K, McLachlan SM, Komorowski L, Luo J, Cabral-Marques O, Hammers CM, Lindstrom JM, Lamprecht P, Fischer A, Riemekasten G, Tersteeg C, Sondermann P, Rapoport B, Wandinger KP, Probst C, El Beidaq A, Schmidt E, Verkman A, Manz RA, and Nimmerjahn F (2017) Mechanisms of Autoantibody-Induced Pathology. Front Immunol 8, 603 [PubMed: 28620373]

24. Atkinson MA, Bluestone JA, Eisenbarth GS, Hebrok M, Herold KC, Accili D, Pietropaolo M, Arvan PR, Von Herrath M, Markel DS, and Rhodes CJ (2011) How does type 1 diabetes develop?: the notion of homicide or beta-cell suicide revisited. Diabetes 60, 1370–1379 [PubMed: 21525508]

25. Arvan P, Pietropaolo M, Ostrov D, and Rhodes CJ (2012) Islet autoantigens: structure, function, localization, and regulation. Cold Spring Harb Perspect Med 2

26. Merriman C, Huang Q, Rutter GA, and Fu D (2016) Lipid-tuned Zinc Transport Activity of Human ZnT8 Protein Correlates with Risk for Type-2 Diabetes. J Biol Chem 291, 26950–26957 [PubMed: 27875315]

27. Zheng SQ, Palovcak E, Armache JP, Verba KA, Cheng Y, and Agard DA (2017) MotionCor2: anisotropic correction of beam-induced motion for improved cryo-electron microscopy. Nat Methods 14, 331–332 [PubMed: 28250466]

28. Rohou A, and Grigorieff N (2015) CTFFIND4: Fast and accurate defocus estimation from electron micrographs. J Struct Biol 192, 216–221 [PubMed: 26278980]

29. Scheres SH (2012) RELION: implementation of a Bayesian approach to cryo-EM structure determination. J Struct Biol 180, 519–530 [PubMed: 23000701]

30. Pettersen EF, Goddard TD, Huang CC, Couch GS, Greenblatt DM, Meng EC, and Ferrin TE (2004) UCSF Chimera--a visualization system for exploratory research and analysis. J Comput Chem 25, 1605–1612 [PubMed: 15264254]

31. Merriman C, Li H, Li H, and Fu D (2018) Highly specific monoclonal antibodies for allosteric inhibition and immunodetection of the human pancreatic zinc transporter ZnT8. J Biol Chem 293, 16206–16216 [PubMed: 30181214]

32. Marx A, Backes C, Meese E, Lenhof HP, and Keller A (2016) EDISON-WMW: Exact Dynamic Programing Solution of the Wilcoxon-Mann-Whitney Test. Genomics Proteomics Bioinformatics 14, 55–61 [PubMed: 26829645]

33. Bonifacio E, Yu L, Williams AK, Eisenbarth GS, Bingley PJ, Marcovina SM, Adler K, Ziegler AG, Mueller PW, Schatz DA, Krischer JP, Steffes MW, and Akolkar B (2010) Harmonization of glutamic acid decarboxylase and islet antigen-2 autoantibody assays for national institute of diabetes and digestive and kidney diseases consortia. J Clin Endocrinol Metab 95, 3360–3367 [PubMed: 20444913]
34. Yu L, Robles DT, Abiru N, Kaur P, Rewers M, Kelemen K, and Eisenbarth GS (2000) Early expression of antiinsulin autoantibodies of humans and the NOD mouse: evidence for early determination of subsequent diabetes. Proc Natl Acad Sci U S A 97, 1701–1706 [PubMed: 10677521]
35. Kodama K, Zhao Z, Toda K, Yip L, Fuhlbrigge R, Miao D, Fathman CG, Yamada S, Butte AJ, and Yu L (2016) Expression-Based Genome-Wide Association Study Links Vitamin D-Binding Protein With Autoantigenicity in Type 1 Diabetes. Diabetes 65, 1341–1349 [PubMed: 26983959]
36. Davidson HW, Wenzlau JM, and O'Brien RM (2014) Zinc transporter 8 (ZnT8) and beta cell function. Trends Endocrinol Metab 25, 415–424 [PubMed: 24751356]
37. Pietropaolo M, Surhigh JM, Nelson PW, and Eisenbarth GS (2008) Primer: immunity and autoimmunity. Diabetes 57, 2872–2882 [PubMed: 18971434]
38. Knip M, Siljander H, Ilonen J, Simell O, and Veijola R (2016) Role of humoral beta-cell autoimmunity in type 1 diabetes. Pediatr Diabetes 17 Suppl 22, 17–24 [PubMed: 27411432]
39. Parikka V, Nanto-Salonen K, Saarinen M, Simell T, Ilonen J, Hyoty H, Veijola R, Knip M, and Simell O (2012) Early seroconversion and rapidly increasing autoantibody concentrations predict prepubertal manifestation of type 1 diabetes in children at genetic risk. Diabetologia 55, 1926–1936 [PubMed: 22441569]
40. Jasinski JM, and Eisenbarth GS (2005) Insulin as a primary autoantigen for type 1A diabetes. Clin Dev Immunol 12, 181–186 [PubMed: 16295523]
41. Liston A, Todd JA, and Lagou V (2017) Beta-Cell Fragility As a Common Underlying Risk Factor in Type 1 and Type 2 Diabetes. Trends Mol Med 23, 181–194 [PubMed: 28117227]
42. Suurmond J, and Diamond B (2015) Autoantibodies in systemic autoimmune diseases: specificity and pathogenicity. J Clin Invest 125, 2194–2202 [PubMed: 25938780]
43. Yu L, Dong F, Miao D, Fouts AR, Wenzlau JM, and Steck AK (2013) Proinsulin/Insulin autoantibodies measured with electrochemiluminescent assay are the earliest indicator of prediabetic islet autoimmunity. Diabetes Care 36, 2266–2270 [PubMed: 23423694]
44. Acevedo-Calado M, James EA, Morran MP, Pietropaolo SL, Ouyang Q, Arribas-Layton D, Songini M, Liguori M, Casu A, Auchus RJ, Huang S, Yu L, Michels A, Gianani R, and Pietropaolo M (2017) Identification of Unique Antigenic Determinants in the Amino Terminus of IA-2 (ICA512) in Childhood and Adult Autoimmune Diabetes: New Biomarker Development. Diabetes Care 40, 561–568 [PubMed: 28174261]
45. Tsuboi T, and Rutter GA (2003) Insulin secretion by 'kiss-and-run' exocytosis in clonal pancreatic islet beta-cells. Biochem Soc Trans 31, 833–836 [PubMed: 12887316]
46. Vo YP, Hutton JC, and Angleson JK (2004) Recycling of the dense-core vesicle membrane protein phogrin in Min6 beta-cells. Biochem Biophys Res Commun 324, 1004–1010 [PubMed: 15485654]
47. Lemaire K, Chimienti F, and Schuit F (2012) Zinc transporters and their role in the pancreatic beta-cell. J Diabetes Investig 3, 202–211
48. Wang D, Eraslan B, Wieland T, Hallstrom B, Hopf T, Zolg DP, Zecha J, Asplund A, Li LH, Meng C, Frejno M, Schmidt T, Schnatbaum K, Wilhelm M, Ponten F, Uhlen M, Gagneur J, Hahne H, and Kuster B (2019) A deep proteome and transcriptome abundance atlas of 29 healthy human tissues. Mol Syst Biol 15, e8503 [PubMed: 30777892]
49. Lemaire K, Ravier MA, Schraenen A, Creemers JW, Van de Plas R, Granvik M, Van Lommel L, Waelkens E, Chimienti F, Rutter GA, Gilon P, in't Veld PA, and Schuit FC (2009) Insulin crystallization depends on zinc transporter ZnT8 expression, but is not required for normal glucose homeostasis in mice. Proc Natl Acad Sci U S A 106, 14872–14877 [PubMed: 19706465]
50. Kambe T, Taylor KM, and Fu D (2021) Zinc transporters and their functional integration in mammalian cells. J Biol Chem, 100320 [PubMed: 33485965]

51. Wang J, Miao D, Babu S, Yu J, Barker J, Klingensmith G, Rewers M, Eisenbarth GS, and Yu L (2007) Prevalence of autoantibody-negative diabetes is not rare at all ages and increases with older age and obesity. J Clin Endocrinol Metab 92, 88–92 [PubMed: 17062766]

52. Krischer JP, Liu X, Vehik K, Akolkar B, Hagopian WA, Rewers MJ, She JX, Toppari J, Ziegler AG, Lernmark A, and Group TS (2019) Predicting Islet Cell Autoimmunity and Type 1 Diabetes: An 8-Year TEDDY Study Progress Report. Diabetes Care 42, 1051–1060 [PubMed: 30967432]

53. Tosur M, Geyer SM, Rodriguez H, Libman I, Baidal DA, Redondo MJ, and Type 1 Diabetes TrialNet Study, G. (2018) Ethnic differences in progression of islet autoimmunity and type 1 diabetes in relatives at risk. Diabetologia 61, 2043–2053 [PubMed: 29931415]

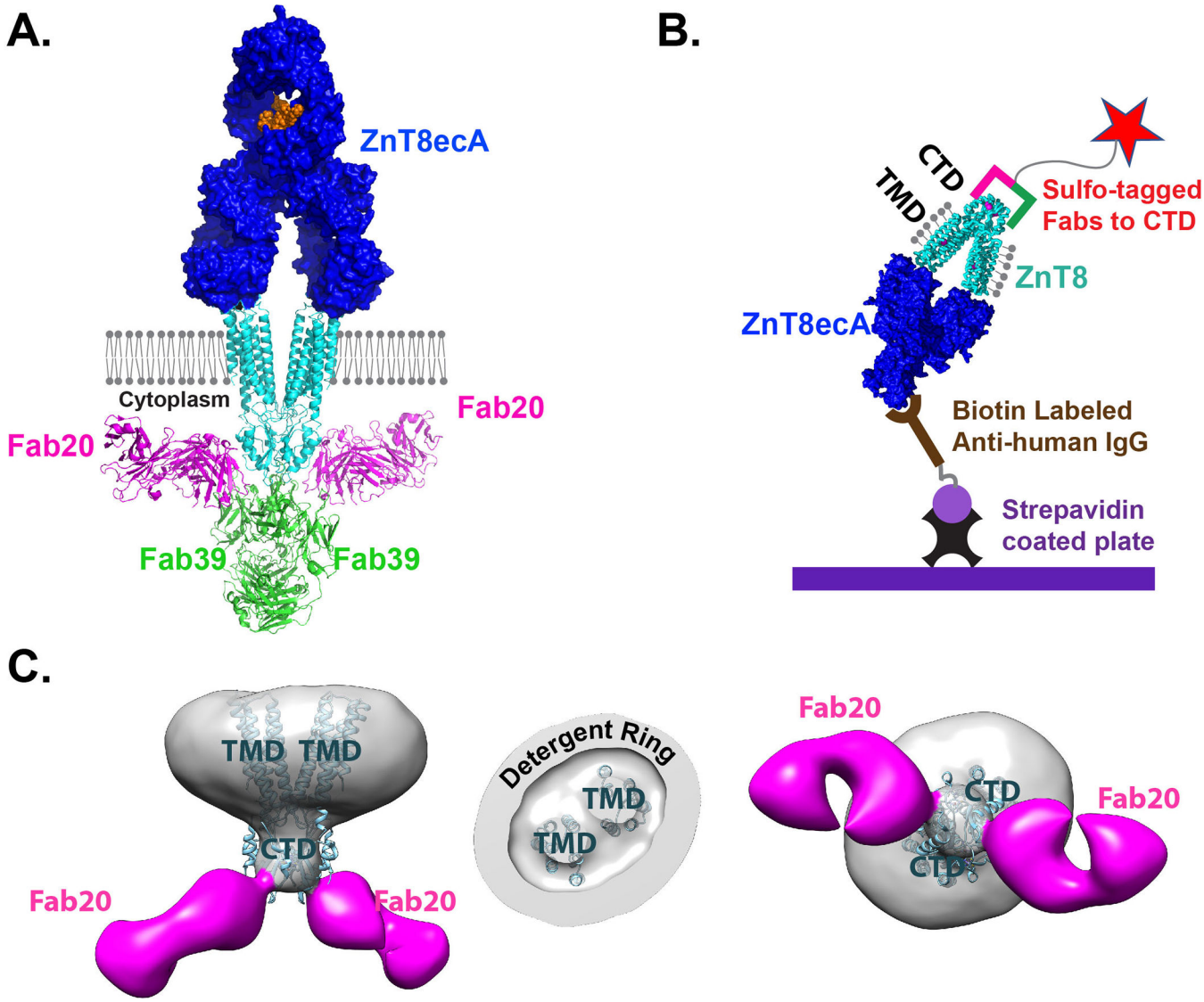

Fig. 1. ZnT8ecA assay on the ECL platform.

A. ZnT8ecA binding to the cell surface and a structural model of ZnT8ecA-ZnT8-Fab20-Fab39 complex in relation to the surface membrane (grey balls and sticks). Proteins are drawn in 1:1 scale in cyan for a ZnT8 homodimer, magenta for Fab20, green for Fab39, blue for a ZnT8ecA in surface representation, and orange for antibody glycosylation. **B.** Schematic diagram of the ECL-assay. ZnT8 was solubilized by detergent (grey balls and sticks), stabilized by Fab (magenta/green bars) conjugated with a sulfo-tag (red star), and captured by a biotinylated anti-IgG secondary antibody via ZnT8ecA binding. **C.** Electron densities of a ZnT8-Fab20 complex with side view, cut-through view of TMDs, and bottom view from the cytoplasmic side. Cyan ribbons are fittings of a human ZnT8 cryo-EM structure to the electron density map.

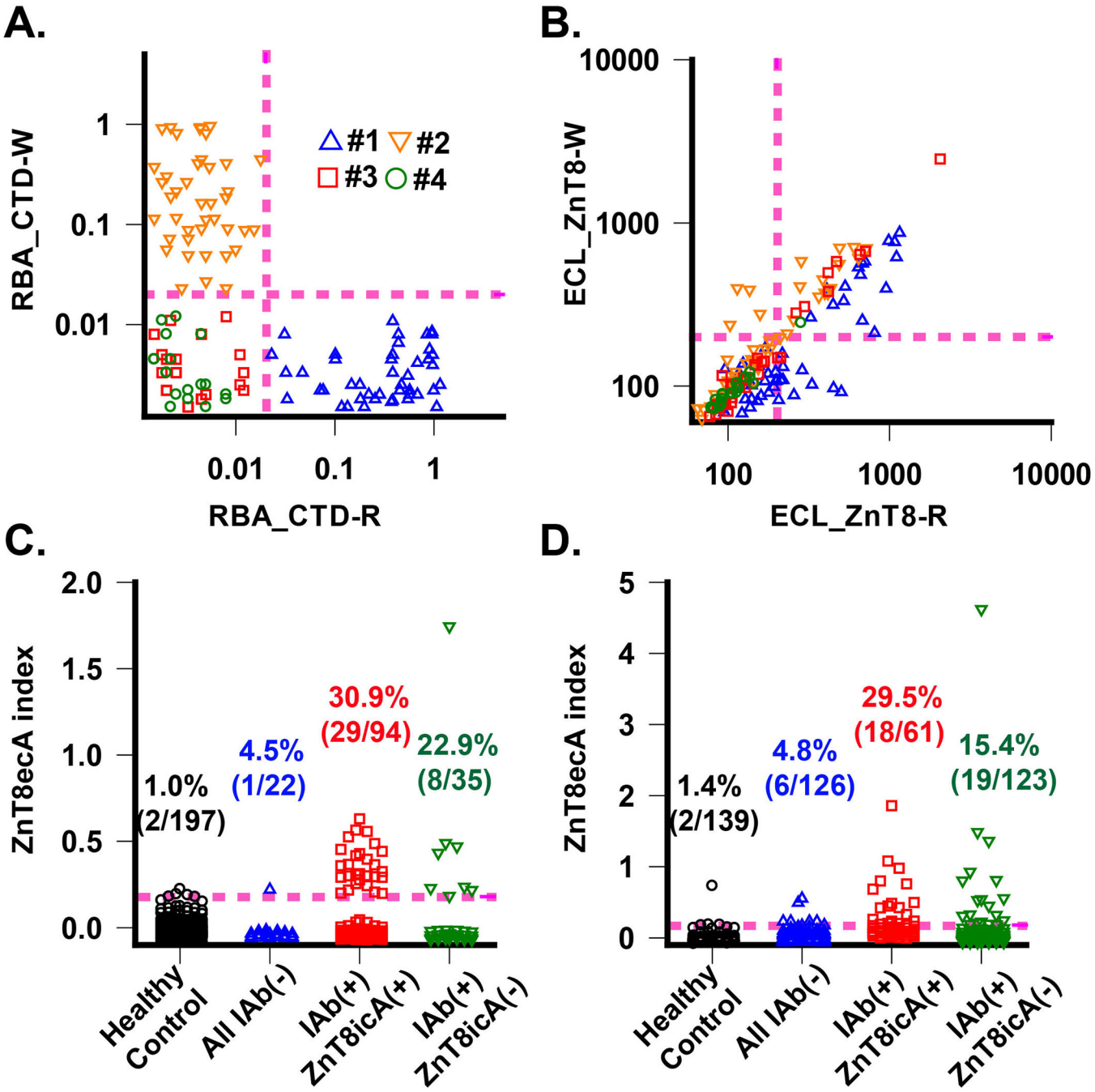

Fig. 2. Detection and validation of ZnT8eAb

A. ZnT8icA by CTD radio-binding assay. ZnT8AicA levels in each serum were measured against CTD-R and CTD-W variants. Datapoints were obtained from fours cohorts of patients with T1D: #1: 49 R-sera with ZnT8icA(+); #2: 45 W-sera with ZnT8icA(+); #3:35 ZnT8icA(–) but other IAb positive; #4: 22 all IAb negative. Magenta dashed lines indicate assay positivity cut-off. **B.** Cross-reaction of ZnT8ecA to ZnT8-R and ZnT8-W. ZnT8ecA levels in each serum were measured against ZnT8-R and ZnT8-W variants in complex with Fab20 and Fab39. Identical patient cohorts were used in **A**. Note, diagonal datapoints

indicate R/W cross-reactivity. **C.** ZnT8ecA positivity in first set of diabetic patient cohorts. The healthy control group was used to determine a positivity cutoff level corresponding to 99% of 197 healthy subjects (magenta dashed line). Diabetic patients were divided into all IAb negative group and IAb positive group, which was further divided into ZnT8icA(+) and ZnT8icA(–) subgroup. **D.** ZnT8ecA positivity in second set of diabetic patient cohorts. The healthy control group was used to determine a positivity cutoff level corresponding to 99% of 139 healthy subjects (magenta dashed line).

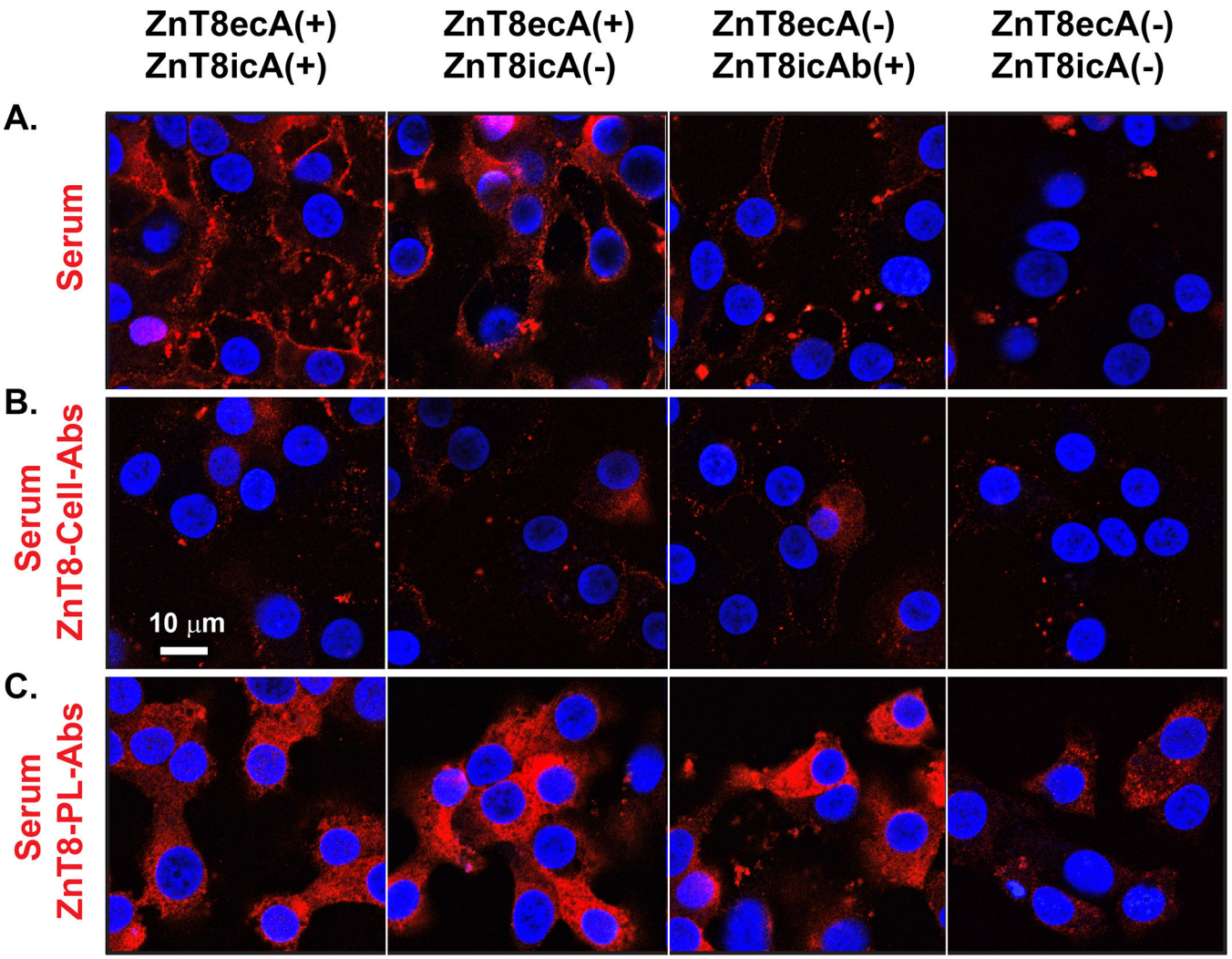

Fig. 3. Cell surface immunofluorescence staining of ZnT8ecA from sera of individual diabetic patients

A. Human EndoC-βH1 cells were exposed to a human serum that was selected for ZnT8ecA and ZnT8icA positive or negative in various combinations as indicated. **B-C.** Identical sera were pre-absorbed by ZnT8-GFP on the surface of intact INS-1E cells (ZnT8-cell-Abs) or by purified human ZnT8 in proteoliposomes (ZnT8-PL-Abs) as indicated. Serum antibodies bound to the cell surface were visualized by confocal microscopy using a secondary antibody against human IgG (red) while cell nuclei were counterstained by DAPI (blue). Representative images are shown from immunofluorescence staining using two independent serum sets, each with 4 replicates.

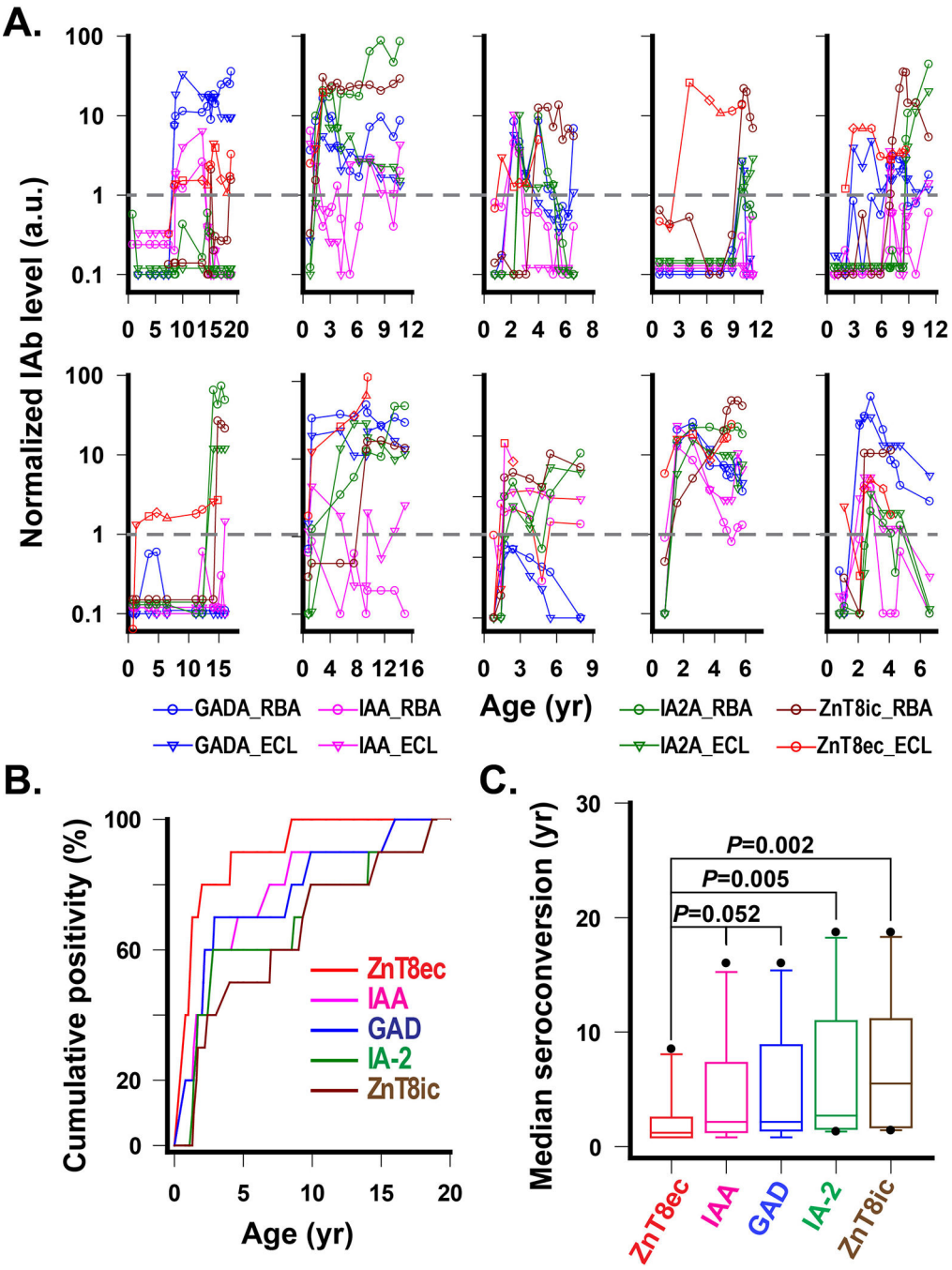

Fig. 4. Temporal responses of IAbs from birth to clinical T1D in 10 DAISY subjects.

A. Time courses of longitudinal IAb levels with a normalized positivity cutoff set to 1.0 (grey dash lines) for all IAbs. **B.** Cumulative IAb positivity from birth to clinical T1D. All subjects (n=10) were monitored for IAb at 9 months of age, then approximately in 3-month intervals until the age of 2, and then 6-month intervals afterward. Note, IAA, GADA and IA-2A were measured by both RBA and ECL assays, and the earliest age points of positive conversions from one of the two assays were selected for this plot. **C.** Median first

seroconversion year for each IAb in 10 DAISY subjects. The *P* values are exact solutions of the two-sided Wilcoxon-Mann-Whitney test for paired data sets (n=10).

Table 1:

Demographic information

	Group 1			Group 2		
	T1DM*	**IAb- DM**	**Control**	**T1DM†**	**IAb- DM**	**Control**
n=	129	22	197	184	126	139
Age (yr):						
mean	12.2	12.8	13.4	13.8	15.7	17.1
median	11.6	13.2	11.5	11.4	13.2	11.7
range	2.0–45.8	1.3–34.8	0.7–51.6	0.7–67.6	1.3–66.8	2.0–51.0
Female (%)	57.4%	50.0%	50.8%	52.6%	45.8%	48.2%

*including 94 patients with ZnT8icA positive and 35 patients negative for ZnT8icA.

†including 123 patients with IAb positive but ZnT8icAb negative, and 61 patients with both IAb and ZnT8icAb positive